

References

1. S. K. Runcorn *et al.*, *Geochim. Cosmochim. Acta* **3** (Suppl. 1), 2369 (1970); *Proc. Roy. Soc. London Ser. A* **325**, 157 (1971); C. E. Helsley, *Geochim. Cosmochim. Acta* **3** (Suppl. 1), 2213 (1970); T. Nagala, R. M. Fisher, F. C. Schwerer, M. D. Fuller, J. R. Dunn, *ibid.* **3** (Suppl. 2), 2461 (1971); D. W. Strangway, G. W. Pearce, E. Larsen, *ibid.* **3** (Suppl. 1), 2435 (1970).
2. P. J. Coleman, G. Schubert, C. T. Russell, L. R. Sharp, *Moon* **4**, 419 (1972); P. Dyal, C. W. Parkin, C. P. Sonett, *Science* **169**, 762 (1970); J. D. Michalov, C. P. Sonett, J. H. Brinscak, M. D. Moutsoulas, *ibid.* **171**, 892 (1971).
3. S. Chapman and J. Bartels, *Geomagnetism* (Oxford Univ. Press, London, 1940).
4. H. C. Urey, K. Marti, J. W. Hawkins, M. K. Liu, *Proceedings of the Second Lunar Science Conference*, A. A. Levinson, Ed. (M.I.T. Press, Cambridge, Mass., 1971), vol. 2, pp. 987-998.
5. H. C. Urey, *The Planets* (Yale Univ. Press, New Haven, Conn., 1952).
6. ———, *Mon. Not. Roy. Astron. Soc.* **131**, 199 (1966).
7. A. S. Eddington, *Internal Constitution of the Stars* (Cambridge Univ. Press, London, ed. 3, 1930).
8. J. Bainbridge, *Astrophys. J.* **136**, 202 (1962).
9. R. G. Ostic, *Mon. Not. Roy. Astron. Soc.* **131**, 191 (1965).
10. B. M. Middlehurst, in *The Moon*, S. K. Runcorn and H. C. Urey, Eds. (Reidel, Dordrecht, Netherlands, 1972), pp. 450-457.
11. H. Alfven, *On the Origin of the Solar System* (Clarendon Press, Oxford, 1954).
12. S. K. Runcorn, in *From Plasma to Planet*, Nobel Symposium 21, A. Elvius, Ed. (Almqvist & Wiksell, Stockholm, 1972), pp. 373-376.
13. C. P. Sonnett, D. S. Colburn, K. Schwartz, *Nature* **219**, 924 (1968).
14. S. K. Runcorn, *Proc. Roy. Soc. Ser. A* **296**, 270 (1967).
15. March 1973

Periodic Insolation Variations on Mars

Abstract. *Previously unrecognized insolation variations on Mars are a consequence of periodic variations in eccentricity, first established by the theory of Brouwer and Van Woerkom (1950). Such annual insolation variations, characterized by both 95,000-year and 2,000,000-year periodicities, may actually be recorded in newly discovered layered deposits in the polar regions of Mars. An additional north-south variation in seasonal insolation, but not average annual insolation, exists with 51,000-year and 2,000,000-year periodicities.*

Unique layered deposits have been discovered in the polar regions of Mars through Mariner 9 photography (1, 2). A history of periodic entrapment, by solid CO₂ deposits on the surface, of dust particles settling out from planet-wide dust storms is likely recorded there. Murray *et al.* (1) postulate that the individual layers might be associated with a 50,000-year alternation in the pattern of insolation at the two poles of Mars previously recognized by

Leighton and Murray (3). A longer-period effect in depositional conditions is indicated by the association of tens of individual layers into distinct overlapping plates. This longer-period effect was ascribed to some unrecognized climatic fluctuation by Murray *et al.* (1).

We report here previously unrecognized long-term periodic variations in the solar insolation reaching Mars (4), which can be expected to regulate the growth and disappearance of perennial

CO₂ deposits and probably also the production of planet-wide dust storms. These insolation variations arise from variations in the eccentricity of the orbit of Mars. This pattern of insolation variations bears a striking similarity to the long-period and short-period fluctuations that seem to be recorded by the layered deposits. Thus, we propose that this newly recognized long-term periodic variation in the insolation, arising from a periodic fluctuation in the eccentricity of the orbit, may be recorded in the polar regions of Mars. A later paper (5) will outline considerations of the actual mechanisms by which this process may have taken place.

Long-term changes in the eccentricity of the orbit of a planet can be computed by using the Laplace-Lagrange theory of secular perturbations. The disturbing function is limited to its secular part; that is, all periodic terms containing the mean longitudes are ignored. This is equivalent to spreading out the mass of each planet in the solar system along its orbit with a local density proportional to the time spent at each position. Since the eccentricities can sometimes become very small, it is convenient to define the following quantities: $h_i = e_i \sin \omega_i$, $k_i = e_i \cos \omega_i$, where e_i and ω_i are the eccentricity and longitude of perihelion, respectively. The pertinent part of the secular disturbing function between two planets p and q thus takes the form

$$\bar{R}_{pq} = \frac{GM^*a_p}{4a_q^3} \left[\frac{1}{2} b_{3/2}^{(1)} (h_p^2 + k_p^2 + h_q^2 + k_q^2) - b_{3/2}^{(2)} (h_p h_q + k_p k_q) \right] \quad (1)$$

and the perturbation equations for h_i and k_i are

$$\frac{dh_i}{dt} = \frac{1}{n_i a_i^2} \frac{\partial \bar{R}_i}{\partial k_i} \quad \frac{dk_i}{dt} = \frac{-1}{n_i a_i^2} \frac{\partial \bar{R}_i}{\partial h_i} \quad (2)$$

where \bar{R}_i is the total secular disturbing function felt by planet i obtained by summing the contributions from all the other planets, n_i is the mean motion, and t is time. In Eq. 1, G is the gravitational constant; a_p and a_q are the semi-major axes, with $a_p < a_q$; and $b_s^{(r)}$ denotes a Laplace coefficient that is a function of a_p/a_q . The mass of the perturbing object is denoted by M^* . Carrying out the differentiation indicated in Eq. 2 yields a system of linear first-order differential equations. The motions of the perihelia and changes in the eccentricities of all the planets are coupled to each other and must be solved for together. A solution has been obtained for the solar system (excluding Pluto) by Brouwer and Van Woerkom

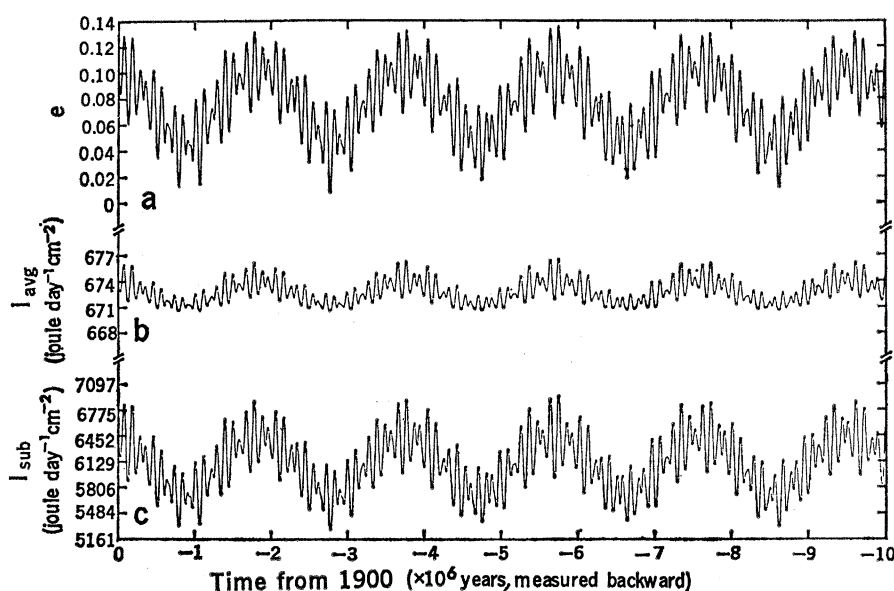


Fig. 1. (a) Eccentricity of Mars for the past 10^7 years; (b) average annual insolation at the poles; (c) insolation at the subpolar point at perihelion.

(6). Eight eigenvalues, S_i , and eigenvectors were found, each being a solution to the system of Eq. 2. In general, h_i and k_i are given by a superposition of the appropriate components of each eigenvector and have the form

$$\begin{aligned} h_i &= \sum_j M_{ij} \cos(-S_j t + \epsilon_j) \\ k_i &= \sum_j M_{ij} \sin(-S_j t + \epsilon_j) \end{aligned} \quad (3)$$

The constants M_{ij} and ϵ_j are ascertained from the values of h_i and k_i in the epoch 1900 (7). The eccentricity can be computed from

$$e_i = (h_i^2 + k_i^2)^{1/2}$$

The upper curve of Fig. 1 shows a plot of the eccentricity of Mars for the past 10^7 years. There are relatively rapid fluctuations with an approximately 95,000-year period during which the eccentricity varies by between .01 and .06. This is superimposed on a much longer, nearly periodic variation every 2×10^6 years. The theoretical maximum possible eccentricity, $e_{\max} = .141$, is obtained by adding the absolute values of all of the coefficients, M_{ij} , and the minimum possible eccentricity, $e_{\min} = .004$, is obtained by subtracting from the largest one the absolute values of all of the remaining coefficients (8). In Fig. 1, a maximum value of only .132 is obtained for the interval shown. However, eccentricities arbitrarily close to the maximum or minimum can be achieved by waiting long enough.

Variations in the perihelion and aphelion distances for the orbit of Mars are due almost solely to the eccentricity fluctuations, since the semimajor axis suffers negligible change on this time scale. Indeed, we are guaranteed, by Poisson's theorem, that there are no secular terms in the expression for the semimajor axis up to second order. It is thus adequate for our purposes to treat the semimajor axis—and therefore the orbital period—as a constant (9).

To numerically relate eccentricity and insolation, we compute the average yearly solar insolation, $\langle I \rangle$, incident at the north pole:

$$\langle I \rangle = \frac{1}{P} \int_0^P S \left(\frac{a}{r} \right)^2 \sin \delta \cos(\phi - \theta) dt \quad (4)$$

$\cos(\phi - \theta) > 0$

where P is the orbital period; δ is the obliquity of Mars; r is the Mars-Sun distance; and ϕ and θ are, respectively, the orbital angular position and longitude of the north hemisphere's summer solstice, to be measured from some fixed inertial space vector lying in the orbit plane. (To the level of our approxima-

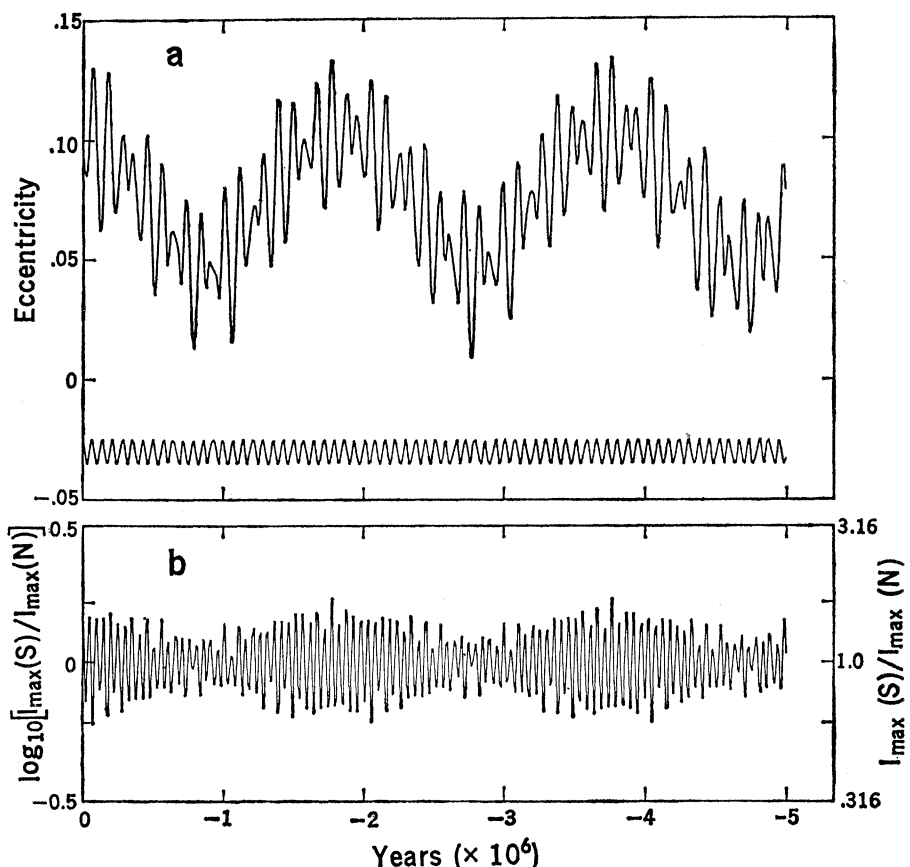


Fig. 2. (a) Eccentricity of Mars and (b) logarithm of the ratio of the maximum polar insulations for 5×10^6 years. Rapid fluctuations in the insolation ratio are due to the 51,000-year beat between the precessing perihelion and spin axis. The longer-period envelope is produced by the 2×10^6 -year periodicity in the eccentricity. For comparison, a plot of $\cos \omega$ [lower curve in (a), without a vertical scale] is included to illustrate the 72,000-year perihelion precession.

tion, we can neglect the inclination of the orbit of Mars to the ecliptic. In this case, we can refer θ and ϕ to the equinox and ecliptic of 1950.) The solar constant, S , has been normalized to a distance of one semimajor axis, a . The integral is taken over all those times during one orbit of period P for which the integrand is positive. Equation 4 can be transformed into an integral over ϕ by Kepler's law, $d\phi/dt = C/r^2$, where $C = 2\pi a^2(1 - e^2)^{1/2}/P$ is a constant. Integration yields

$$\langle I \rangle = \frac{S \sin \delta}{\pi(1 - e^2)^{1/2}} \quad (5)$$

Using the values for Mars, $\delta = 23^\circ 59'$ and $S = 0.06$ watt cm^{-2} , we find that as the eccentricity varies from .004 to .141 the annual average insolation at the geometric pole on Mars varies about 1 percent. This is sufficient, under some conditions, to significantly affect the behavior of permanent CO_2 there. We are also interested in the insolation at the subsolar point at perihelion, $I_{\text{sub}} = S/(1 - e)^2$, which now can be seen to vary as much as 30 percent due to the eccentricity variations. These

relationships are presented in the middle and lower curves of Fig. 1 (10).

Another property of interest is the difference between maximum insolation at the north and south poles for a given orbit. Although the average annual insolation is identical, there does exist an alternating seasonal difference between north and south, that is, a cool fall versus a warm fall. Because of the precession of Mars' spin axis, the precession of the perihelion within the orbital plane, and the previously discussed periodic variations in the eccentricity, the ratio of maximum insolation at the south pole to that at the north pole, $I_{\max}(S)/I_{\max}(N)$, experiences a periodic variation. The insolation at the north pole is given by the integrand of Eq. 4,

$$I(N) = \frac{S \sin \delta}{(1 - e^2)^2} [1 + e \cos(\phi - \omega)]^2 \cos(\phi - \theta) \quad (6)$$

where we have expressed r as a function of ϕ . To first-order accuracy in the eccentricity, the maximum insolation is achieved when $\phi = \theta$ and

$$I_{\max}(N) \cong S \sin \delta [1 + 2e \cos(\theta - \omega)] \quad (7)$$

On the other hand, the insolation at the south pole becomes a maximum when $\phi = \theta + \pi$ and

$$I_{\max}(S) \cong S \sin \delta [1 - 2e \cos(\theta - \omega)] \quad (8)$$

From Eqs. 7 and 8 and the definitions of h and k ,

$$\frac{I_{\max}(S)}{I_{\max}(N)} \cong 1 - 4e \cos(\theta - \omega) \\ = 1 - 4k \cos \theta - 4h \sin \theta \quad (9)$$

The present position of the Mars spin axis and its precession period of 1.75×10^5 years determined by Lorell *et al.* (11) can be used to compute θ as a function of time. A present value of $\theta = 172^\circ$ was taken as sufficiently accurate for our purposes. Figure 2 is a plot of the logarithm of Eq. 9. The maximum polar insolation can be seen to alternate between the north and south poles with a 51,000-year period, and to exhibit a 2,000,000-year periodicity in amplitude, ranging from about 10 percent difference to 50 percent difference. This periodic insolation difference may be important in processes that are nonlinearly related to insolation, such as the mobilization of water vapor from ground ice and certain kinds of atmospheric dynamics.

Thus, it is an intriguing possibility that the insolation of Mars experiences periodic fluctuations on a time scale and of sufficient magnitude to be recorded in at least polar deposits on Mars, especially the layered terrains described by Murray *et al.* (1). In addition, Briggs (12) has shown that the eccentricity variations represented in Fig. 1 probably cause the maximum annual insolation on Mars to sometimes exceed and sometimes not exceed a critical threshold apparently necessary for the generation of a planet-wide dust storm. Thus, periodic insolation variations on Mars may be recorded in sedimentary deposits throughout the planet.

BRUCE C. MURRAY

WILLIAM R. WARD, SZE C. YEUNG*
Division of Geological and Planetary
Sciences, California Institute of
Technology, Pasadena 91109

References and Notes

1. B. C. Murray, L. A. Soderblom, J. A. Cutts, R. P. Sharp, D. J. Milton, R. B. Leighton, *Icarus* 17, 328 (1972).
2. L. A. Soderblom, M. C. Malin, J. A. Cutts, B. C. Murray, R. P. Sharp, *J. Geophys. Res.*, in press; B. C. Murray and M. C. Malin, *Science* 179, 997 (1973); J. A. Cutts, *J. Geophys. Res.*, in press.
3. R. B. Leighton and B. C. Murray, *Science* 153, 136 (1966). Leighton and Murray argued that the average annual insolation at each pole varied with a 50,000-year period. H. H. Kieffer (private communication) has shown that this is not correct for the average annual insolation; however, we show here that such a periodicity exists in the maximum annual insolation.

4. A very-long-period secular increase on the billion-year time scale of the solar luminosity has been postulated by Sagan [C. Sagan, "The long winter model of martian biology: A speculation" (paper No. 455, Center for Radiophysics and Space Research, Cornell University, Ithaca, N.Y., 1971)]. That effect is not relevant to the present discussions, since the laminated deposits observed are of a much younger age.
5. B. C. Murray and M. C. Malin, in preparation.
6. D. Brouwer and A. J. J. Van Woerkom, *Astron. Pap. Amer. Ephemeris Naut. Alm.* 13 (part 2), 81 (1950).
7. The accuracy of the solution was improved by Brouwer and Van Woerkom (6) by including the effect of one periodic term in the disturbing function—the great inequality between Jupiter and Saturn, which has a period of about 900 years. This adds two terms to h and k for Mars, with arguments corresponding to $2S_6 - S_8$ and $2S_8 - S_6$.
8. D. Brouwer and G. M. Clemence, *Planets and Satellites* (Univ. of Chicago Press, Chicago, 1961), p. 50.
9. In a manner completely analogous to that described for the eccentricity, the secular variations of the inclinations of the planetary orbit planes were also obtained by Brouwer and Van Woerkom (6). It was found that the inclination of the orbit of Mars could vary from 0° to 6.5° . However, the effect of this variation on the obliquity of Mars is not immediately apparent. This is because of the possibility of a coupling between the motion of the orbit normal and the 175,000-year precession of the Mars spin axis due to the torque exerted by the sun on the equatorial bulge of the planet. It can be shown that if the orbit normal moves through inertial space

slowly compared to the motion of the spin axis, the obliquity tends to remain nearly constant [W. R. Ward, thesis, California Institute of Technology (1972)]. However, when the rates of these two motions are comparable, the time variation of the obliquity is more complicated. Brouwer and Van Woerkom found both short-period and long-period fluctuations in the inclination similar to those characterizing the eccentricity. It should be emphasized, however, that a change in the obliquity can occur from the rotation of the nodes alone. Since changes in the average polar insolation are dependent to first order on variations in the obliquity, while only to second order on variations in the eccentricity, it is possible that obliquity variational effects dominate those described in this report. This is a problem that deserves further treatment.

10. Through a reviewer we have learned that a similar computation has been carried out by C. J. Cohen, E. C. Hubbard, and C. Oesterwinter (*Celestial Mech.*, in press).
11. J. Lorell *et al.*, *Icarus*, in press.
12. G. A. Briggs, private communication.
13. L. A. Soderblom of the U.S. Geological Survey and California Institute of Technology originally called our attention to the Brouwer and Clemence reference to Mars' eccentricity variations, the essential starting point for this investigation. P. Goldreich of California Institute of Technology provided helpful advice. This work was partly supported by the National Aeronautics and Space Administration, Contribution No. 2235, Division of Geological and Planetary Sciences, California Institute of Technology.

* Present address: Physics Department, Princeton University, Princeton, New Jersey 08540.

24 November 1972; revised 14 February 1973 ■

Genetic Mapping of the Fv-1 Locus of the Mouse

Abstract. The Fv-1 locus of the mouse, a major determinant of the biology of murine leukemia virus, is very closely linked to Gpd-1 on chromosome 4 (linkage group VIII).

The Fv-1 locus of the mouse (1) is the major determinant of the sensitivity of mouse cells, in vivo or in vitro, to infection with naturally occurring strains of murine leukemia virus (MuLV) (2). Indirect evidence suggests that Fv-1 type also has a strong influence on the incidence of spontaneous lymphoma in hybrids between high and low leukemic mouse strains, presumably as a result of its effect on cell-to-cell spread of virus (3). In the backcross to AKR from crosses between the high virus AKR mouse strain (Fv-1ⁿ) and low virus strains carrying the Fv-1^b allele, which is restrictive for the murine leukemia virus contributed by AKR, inheritance of the Fv-1ⁿ allele is strongly

correlated with expression of infectious virus (3), the MuLV group-specific (gs) antigen, and the G_{IX} antigen of thymocytes (4). In the case of infectious virus, Fv-1 regulates expression by determining the sensitivity or resistance of the cells to spread of infection; in the case of G_{IX} antigen, the correlation of antigen expression with Fv-1 type appears to result from linkage (4). Thus, the Fv-1 locus is of major importance in the biology of murine leukemia, and its precise localization in the mouse genome could be important for the study of mouse neoplasia.

We have recently found (5) that Fv-1 is on chromosome 4 (linkage group VIII), since segregation analysis

Table 1. Three-point cross of *b*, Fv-1, and Gpd-1; (C57BL/6J × DBA/2J) × DBA/2N and reciprocal mating. All mice have one chromosome of genotype: *b* Fv-1ⁿ Gpd-1^b; the other chromosome is that given in the table. The recombination frequencies ± the standard error are: *b* to Fv-1: 39/107 = 36.4 ± 4.7 percent; Fv-1 to Gpd-1: 1/107 = 0.9 ± 0.9 percent; and *b* to Gpd-1: 40/107 = 37.4 ± 4.7 percent.

Item	Parental	Recombinant <i>b</i> to Fv-1	Recombinant Fv-1 to Gpd-1	Double recombinant
Genotype	<i>b</i> Fv-1 ⁿ Gpd-1 ^b	<i>b</i> Fv-1 ^b Gpd-1 ^a	<i>b</i> Fv-1 ⁿ Gpd-1 ^a	<i>b</i> Fv-1 ^b Gpd-1 ^b
No. of mice	30	24	0	0
Genotype	<i>B</i> Fv-1 ^b Gpd-1 ^a	<i>B</i> Fv-1 ⁿ Gpd-1 ^b	<i>B</i> Fv-1 ^b Gpd-1 ^b	<i>B</i> Fv-1 ⁿ Gpd-1 ^a
No. of mice	37	15	1	0